remote sensing

MDPI

Article

An Analysis Study of FORMOSAT-7/COSMIC-2 Radio Occultation Data in the Troposphere

Shu-Ya Chen [1], Chian-Yi Liu [1,2,3,*], Ching-Yuang Huang [1,3], Shen-Cha Hsu [3], Hsiu-Wen Li [1], Po-Hsiung Lin [4], Jia-Ping Cheng [5] and Cheng-Yung Huang [6]

1 GPS Science and Application Research Center, National Central University, Taoyuan 32001, Taiwan; shuyachen@ncu.edu.tw (S.-Y.C.); hcy@atm.ncu.edu.tw (C.-Y.H.); ncu65565@ncu.edu.tw (H.-W.L.)
2 Center for Space and Remote Sensing Research, National Central University, Taoyuan 32001, Taiwan
3 Department of Atmospheric Sciences, National Central University, Taoyuan 32001, Taiwan; sc104621022@g.ncu.edu.tw
4 Department of Atmospheric Sciences, National Taiwan University, Taipei 10617, Taiwan; polin@ntu.edu.tw
5 Central Weather Bureau, Taipei 10048, Taiwan; olga@cwb.gov.tw
6 National Space Organization, National Applied Research Laboratories, Hsinchu 30078, Taiwan; yusn@nspo.narl.org.tw
* Correspondence: cyliu@g.ncu.edu.tw; Tel.: +886-3-4227151 (ext. 57618)

Abstract: This study investigates the Global Navigation Satellite System (GNSS) radio occultation (RO) data from FORMOSAT-7/COSMIC-2 (FS7/C2), which provides considerably more and deeper profiles at lower latitudes than those from the former FORMOSAT-3/COSMIC (FS3/C). The statistical analysis of six-month RO data shows that the rate of penetration depth below 1 km height within ±45° latitudes can reach 80% for FS7/C2, significantly higher than 40% for FS3/C. For verification, FS7/C2 RO data are compared with the observations from chartered missions that provided aircraft dropsondes and on-board radiosondes, with closer observation times and distances from the oceanic RO occultation over the South China Sea and near a typhoon circulation region. The collocated comparisons indicate that FS7/C2 RO data are reliable, with small deviations from the ground-truth observations. The RO profiles are compared with collocated radiosondes, RO data from other missions, global analyses of ERA5 and National Centers for Environmental Prediction (NCEP) final (FNL), and satellite retrievals of NOAA Unique Combined Atmospheric Processing System (NCAPS). The comparisons exhibit consistent vertical variations, showing absolute mean differences and standard deviations of temperature profiles less than 0.5 °C and 1.5 °C, respectively, and deviations of water vapor pressure within 2 hPa in the lower troposphere. From the latitudinal distributions of mean difference and standard deviation (STD), the intertropical convergence zone (ITCZ) is evidentially shown in the comparisons, especially for the NUCAPS, which shows a larger deviation in moisture when compared to FS7/C2 RO data. The sensitivity of data collocation in time departure and spatial distance among different datasets are presented in this study as well.

Keywords: FORMOSAT-7/COSMIC-2; GNSS RO; verification

Citation: Chen, S.-Y.; Liu, C.-Y.; Huang, C.-Y.; Hsu, S.-C.; Li, H.-W.; Lin, P.-H.; Cheng, J.-P.; Huang, C.-Y. An Analysis Study of FORMOSAT-7/COSMIC-2 Radio Occultation Data in the Troposphere. *Remote Sens.* **2021**, *13*, 717. https://doi.org/10.3390/rs13040717

Academic Editor: Stefania Bonafoni
Received: 11 December 2020
Accepted: 12 February 2021
Published: 16 February 2021

1. Introduction

FORMOSAT-3/COSMIC (FS3/C, hereafter FS3), with cross-links to the Global Navigation Satellite System (GNSS), has provided more than six million radio occultation (RO) soundings during the past fourteen years. Many studies have demonstrated the benefits of GNSS RO data on numerical weather predictions and climate change studies, as overviewed by [1]. The GNSS RO data can provide valuable information about the vertical variations in the ionosphere and lower atmosphere, and FS3 has contributed most of the RO measurements since launch in 2006. The advantages of GNSS RO data rely on their highly accurate retrieval of the temperature in the upper troposphere and lower stratosphere (UTLS) (e.g., [2–5]). However, a challenge remains the demanding improvement for RO

data to be applied to the lower troposphere over the tropical region, mainly due to the difficulty in reliable retrievals under large vertical moisture variations [1].

The FORMOSAT-7/COSMIC-2 (FS7/C2, hereafter FS7) project is the follow-on mission of FS3, with six satellites operated in the orbits of lower inclination (24°) to provide more RO data over the lower-latitude regions (± 45° latitudes). Besides the different data coverage, the FS7 satellites are capable of receiving signals from both the Global Positioning System (GPS) and Globalnaya Navigatsionnaya Sputnikovaya Sistema (GLONASS) [6]. FS7 satellites carry an antenna with a higher signal-to-noise ratio (SNR), which thus allows a deeper penetration of the ray into the lower troposphere and better detection of the atmospheric boundary layer (ABL) top and super-refraction (SR) on top of the ABL [7]. The six satellites of the FS7 constellation were successfully launched on 25 June 2019, and the FS7 neutral atmosphere data were officially released on 10 December 2019. There are 4000–5000 RO soundings per day for FS7, which can be accessed from the two RO data processing centers, i.e., the COSMIC Data Analysis and Archive Center (CDAAC) and the Taiwan Analysis Center for COSMIC (TACC).

The RO signal can be retrieved for the upstream data format and bending angle, which then can be reverted to refractivity using Abel inversion. With auxiliary data from other observations or global analysis, atmospheric temperature, and moisture soundings can be retrieved from the RO refractivity (see [8]). Retrievals of both RO bending angle and refractivity can be termed "dry products" (used to obtain the dry temperature) in CDAAC before blending the auxiliary data with the retrievals using 1-D variational minimization to obtain the wet temperature and moisture. The reliability of FS3 RO retrieval was reported in [9]. Applications of FS3 RO data to many aspects of weather prediction and analysis can be found in a number of literatures and have been documented in detail by [1]. The authors of [7] compared the FS7 RO data with different datasets and showed that the FS7 data possess high accuracy and precision. For example, they compared the FS7 RO dry products (bending angle and refractivity) with the European Centre for Medium-Range Weather Forecasts (ECMWF) short-term forecasts and showed that the RO data are quite consistent, with very small biases between 6 and 40 km. However, some larger negative biases are presented below 2 km and smaller positive biases are presented between 2 and 6 km. The negative biases in the lower troposphere may be caused by SR, tracking depth and noise, and fluctuations of refractivity, etc., as discussed in [9]. The authors of [10] compared FS7 RO refractivity with Vaisala RS41 radiosonde data, which is currently the most accurate radiosonde observation and showed a negative difference in the lower troposphere. The negative biases further transfer to the RO wet products (the descendant data) after One-Dimensional Variational (1DVAR) retrieval (https://cdaac-www.cosmic.ucar.edu/cdaac/doc/documents/1dvar.pdf). The 1DVAR retrieval algorithm derives optimal atmospheric temperature, pressure, and humidity profiles according to the RO refractivity and a priori atmospheric state from the numerical model. As described in [1], quantification of the accuracy for RO-derived water vapor is essential for climate studies.

In this study, we aimed to conduct further analyses of the FS7 RO wet retrievals (i.e., wetPf2). For illustrating the properties of FS7 RO retrievals in the troposphere, the wet RO retrievals are compared with multiple datasets, including dropsondes, radiosondes, global analyses, and satellite retrieval data. We also compare the FS3 and FS7 RO retrievals for their data discrepancies in the horizontal and vertical distributions. A brief introduction of the FS7 RO data and other datasets used in this study is given in Section 2. Special dropsondes and radiosondes provided by two chartered missions, presented in Section 3, are used as ground-truth observations for verification on FS7 RO data. Then, the statistical comparisons with different datasets in a six-month period are discussed. Finally, the conclusions are given in Section 4.

2. Data and Methodology

Several satellite missions carried GNSS data receivers, for example, Taiwan–US FS3 and FS7, European Organization for the Exploitation of Meteorological Satellites (EUMETSAT) GRAS (GPS Receiver for Atmospheric Sounding) on the Metop (Meteorological Operational satellites program), and Korea Multi-Purpose Satellite-5 (KOMPSAT-5) provide abundant GNSS RO soundings. To detect the data characteristics of the FS7 RO soundings, the radiosonde observations (RAOB) derived from the National Center for Atmospheric Research (NCAR) Research Data Archive and collocated with the FS7 occultation profiles were derived for the verification. In addition, two special observation missions that provide dropsondes (DROP) and radiosondes observations were chartered for the FS7 verification. Multiple datasets, including global analyses and satellite retrievals, were used for comparison as well. The spatiotemporal windows defined for the collocation were ±3 h and ±100 km of the RO event. The global analyses include the National Centers for Environmental Prediction (NCEP) final (FNL) analysis [11] and the fifth generation of ECMWF atmospheric re-analyses of the global climate (ERA5) ([12]), and both resolutions are in 0.25° latitude and longitude grids. The satellite retrievals from NOAA Unique Combined Atmospheric Processing System (NUCAPS) data were used for comparison. The time period for the statistical comparison was from October 2019 to March 2020 (6 months).

2.1. GNSS RO Data from FS3 and FS7

The FS3 constellation is on an orbit of high inclination (72°) that generates more observations at higher latitudes but still globally distributed. In contrast, the FS7 constellation is on an orbit of low inclination (24°), and most of the RO data are located within ±45º latitudes. FS7 can provide about 4000–5000 RO soundings per day, which is about twice the FS3 RO data. Figure 1 shows the RO data density for one month in 2.5° × 2.5° bins within ±45° latitudes for FS3 in March 2009 and FS7 in March 2020. Significant differences in the RO density appear in the tropical region. FS3 shows a nearly homogeneous data density in the subtropical region but with less data in the tropical region. In contrast, the FS7 has a higher data density over the tropical region because of the low-inclination orbit, and some satellites have not moved to the final orbit height yet. Generally, the data density for FS3 is less than 20 RO profiles in the subtropics and even fewer data near the equator. For FS7, there are about 50–60 RO profiles in the tropical region, considerably more than the FS3.

FS7 with a higher SNR is expected to increase the capability of the ray, reaching lower altitudes. As one example of the comparison on one day, Figure 2 shows the FS3 data on 5 February 2009 and FS7 on 5 February 2020, with their lowest penetrative heights indicated. There are 1018 RO soundings from FS3 and 5419 RO soundings from FS7 in the region of ±45° latitudes. Every dot point in Figure 2 indicates one RO sounding, and the color indicates the lowest height for each sounding. Note that all of the altitudes for the penetration in the figure were measured above the surface. Figure 2 illustrates that most of the FS7 RO data extend deeper into the lower troposphere than FS3. For example, the penetrative depths of FS7 data are below 1 km (Figure 2b), compared to about 1–2 km for the FS3 data (Figure 2a). The distribution of penetrative depths can be clearly seen from the 6-month statistical histogram (Figure 3). The data were collected from October 2008 to March 2009, with 209,709 RO profiles for FS3, and from October 2019 to March 2020, with 599,676 RO profiles for FS7. The data amounts for FS7 are about three times than that for FS3. All the lowest heights were stratified by a 500-m interval until 6 km, and the penetrative depth above 6 km was counted at heights of 5.5–6 km intervals. Figure 3 shows that the penetrative depths of RO soundings for FS3 mostly reach 0.5–1.5 km height, while FS7 gives the highest percentage in the altitude below 0.5 km. Statistically, the rate of penetration below 1 km is about 40% for FS3 and 80% for FS7. Similar statistical results are also found in [7,10].

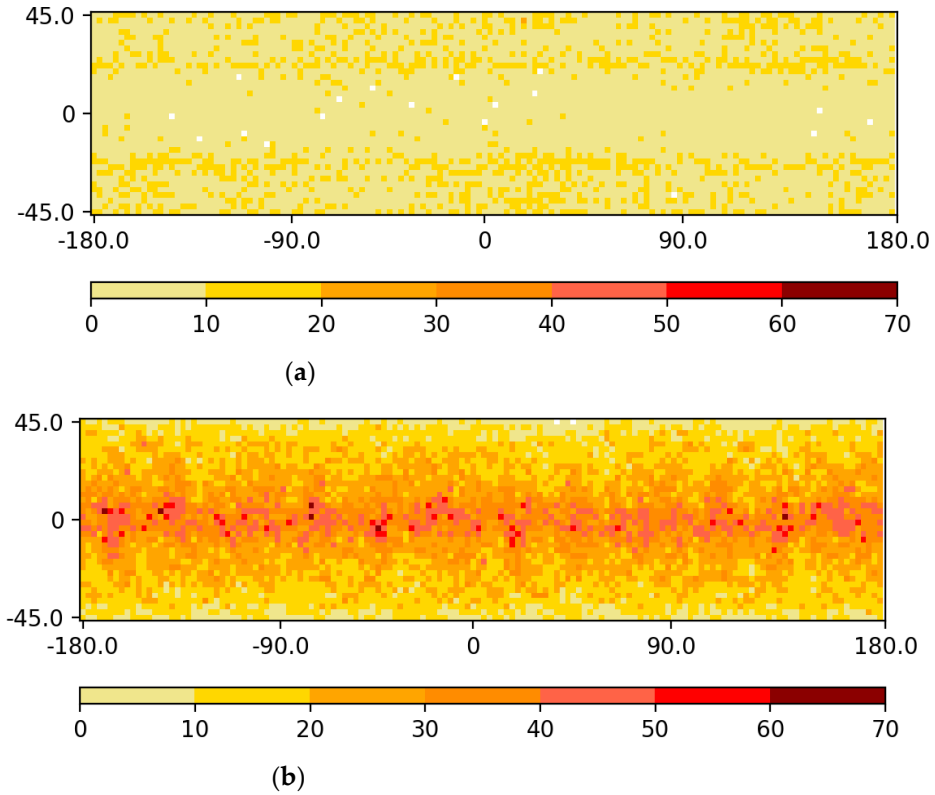

Figure 1. The data density of radio occultation soundings for (**a**) FORMOSAT-3 in March 2009 and (**b**) FORMOSAT-7 in March 2020. The data are counted on 2.5° by 2.5° bins.

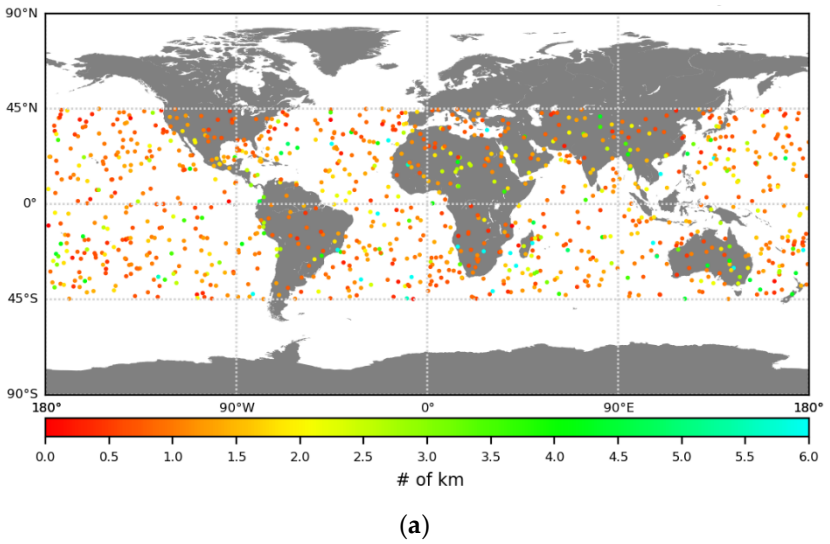

Figure 2. *Cont.*

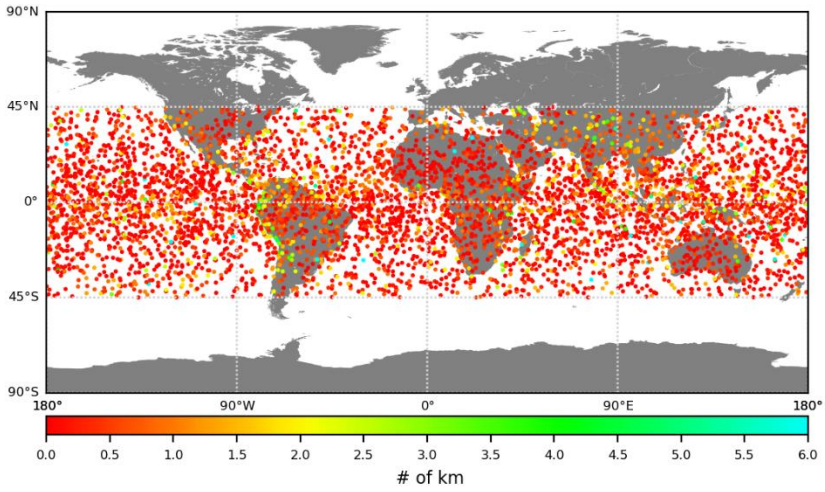

(**b**)

Figure 2. The radio occultation (RO) soundings within ±45° latitudes (**a**) for FORMOSAT-3 on 5 February 2009 and (**b**) for FORMOSAT-7 on 5 February 2020. The color indicates the lowest penetration height (km) of each RO sounding above the surface.

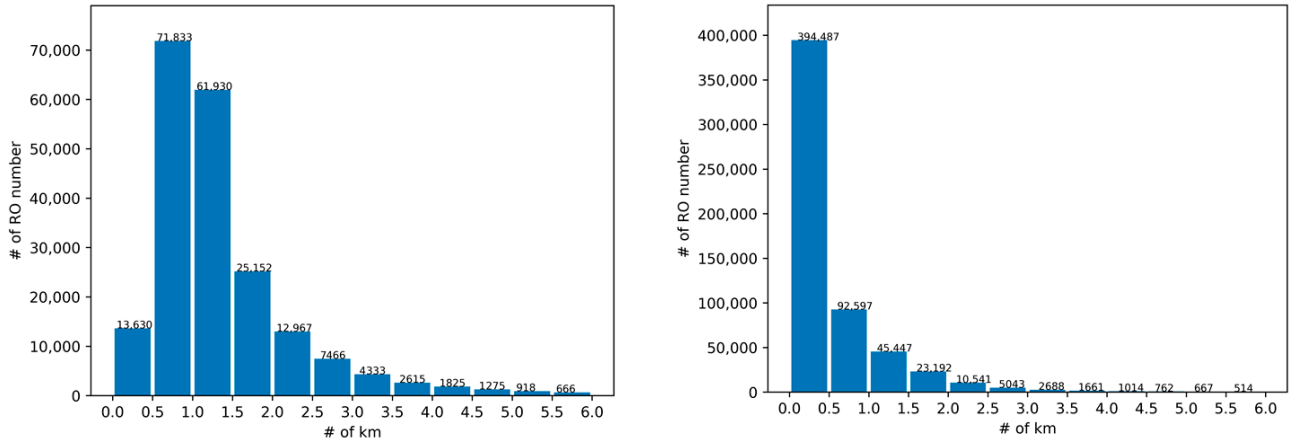

Figure 3. Data count of RO penetrative depth with a 500-m interval (**a**) for FORMOSAT-3 from October 2008 to March 2009 and (**b**) for FORMOSAT-7 from October 2019 to March 2020. All the heights are measured above the surface.

2.2. Data for Verification

Another two RO datasets, i.e., Metop and KOMPSAT-5 RO data, were chosen for inter-comparisons with the FS7 RO data. The Metop RO data were processed by the Radio Occultation Meteorology Satellite Application Facility (ROM SAF) and KOMPSAT-5 by the CDAAC. The Metop series includes three polar-orbiting satellites, Metop-A, B, and C, operated by the EUMETSAT, and there are about 500–600 RO profiles per day globally from each satellite [13]. The Metop RO (hereafter METOP) data show a negative bias in the bending angle in the lower troposphere that increases with lower latitudes when compared to the ECMWF forecast and FS3 [14]. The authors of [15] demonstrated that the negative differences between FS3 and METOP are related to the different tracking depths (FS3 has deeper data) and data retrieval methods. The KOMPSAT-5 RO products are processed by University Corporation for Atmospheric Research (UCAR) and can provide about 500 RO soundings daily. A large difference, in the range of 7 to 13 km altitude, was reported when comparing results from KOMPSAT-5 rising occultation and NCEP forecast. The issue is still under investigation, and UCAR recommends using only the setting occultations by the

moment [16]. The KOMPSAT-5 data have comparable data quality to that of FS3 [17]. Since the KOMPSAT-5 rising occultations were flagged as bad, only the KOMPSAT-5 setting occultations with a good flag of about 200 profiles per day are wesed for the verifications. Hereafter, the KOMPSAT-5 RO data used in this study are indicated as KOMP5.

The three-dimensional global analyses included the ERA5 reanalysis and the NCEP FNL operational global analysis. The ERA5 provides data with a horizontal resolution of 30 km and 137 vertical levels from surface up to 80 km height. The NCEP FNL data were obtained from the NCAR Research Data Archive, with a horizontal resolution of 0.25°. Note that the NCEP FNL data were derived through the Global Data Assimilation System (GDAS) and covered the vertical range from surface to 10 hPa. Both the ERA5 and NCEP FNL possess high horizontal resolution adequate for the comparison. Both the analyses were interpolated into the locations of collocated FS7 RO soundings. ECMWF started assimilating FS7 RO data from 25 March 2020 [18], and only a few days overlapped with the statistical period in this study. For NCEP FNL, there was no overlapped time for the RO data analysis in this study since the FS7 RO data was assimilated at NCEP after 26 May 2020 [19]. Thus, most of the RO data information from FS7 is not repeated in both global analyses.

Other than the data mentioned previously, the retrieved atmospheric temperature and moisture sounding profiles from advanced passive microwave and hyperspectral infrared sensors were adopted for the intercomparison as well. NUCAPS is the NOAA operational satellite sounding retrieval algorithm for microwave and infrared sounders onboard Suomi National Polar-orbiting Partnership (SNPP) and NOAA-20 satellites. NUCAPS was also used to retrieve data from the Joint Polar Satellite System-1 (JPSS1) (renamed as NOAA-20 after Nov. 2017). The atmospheric soundings are retrieved from the synesthetic use of the Cross-track Infrared Sounder (CrIS) and Advanced Technology Microwave Sounder (ATMS), which have 1305 and 22 channels in infrared and microwave spectral regions, respectively [20]. The sound profiles contain more than 100 pressure levels from surface to the 0.005 hPa, with uncertainties of about 1 K and 20% in temperature and moisture mixing ratio in the troposphere from the NUCAPS Algorithm Theoretical Basis Document (ATBD). These data have been supported for both operational applications and research studies (e.g., [21–23]).

Within the six months, Figure 4 shows the daily data amounts of different datasets corresponding to the matching criteria for collocated RO points. There are about one hundred data pairs per day for comparison with METOP, and much fewer pairs for the RAOB and KOMP5 RO data (Figure 4). Each METOP satellite (A, B, and C) gives about three-thousands RO soundings matched with FS7 in the six months. From temporal and spatial interpolation, the global analyses give the exact same amounts paired with the FS7 RO data. The JPSS1 and SNPP satellite data are the second largest for paring data. Because JPSS1 and SNPP were launched on the same orbit and pass the same location within 50 min, a superposition can be seen in Figure 4. Daily data amounts after paring do not considerably vary with time during the six months, except for a larger drop in the first two weeks of November 2019. That was caused by the scheduled orbit adjustment of FS7 satellites in that period. For RAOB and KOMP5, there are some occasions at specific times without collocated RO data as both datasets provide relatively fewer data amounts compared to other datasets.

The multiple datasets were evaluated by mean difference (μ) and standard deviation (STD, σ) with respect to the reference data for comparison or verification. The mean difference and STD were calculated, respectively, as

$$\mu = \frac{1}{num} \sum_{i=1}^{num} x_i \text{ with } x_i = dataset_i - FS7_i \quad (1)$$

$$\sigma = \sqrt{\frac{1}{num} \sum_{i=1}^{num} (x_i - \mu)^2} \quad (2)$$

where $dataset_i$ and $FS7_i$ indicate multiple datasets and the FS7 RO used for the verification or comparison, and i is a data point of total num data during the period.

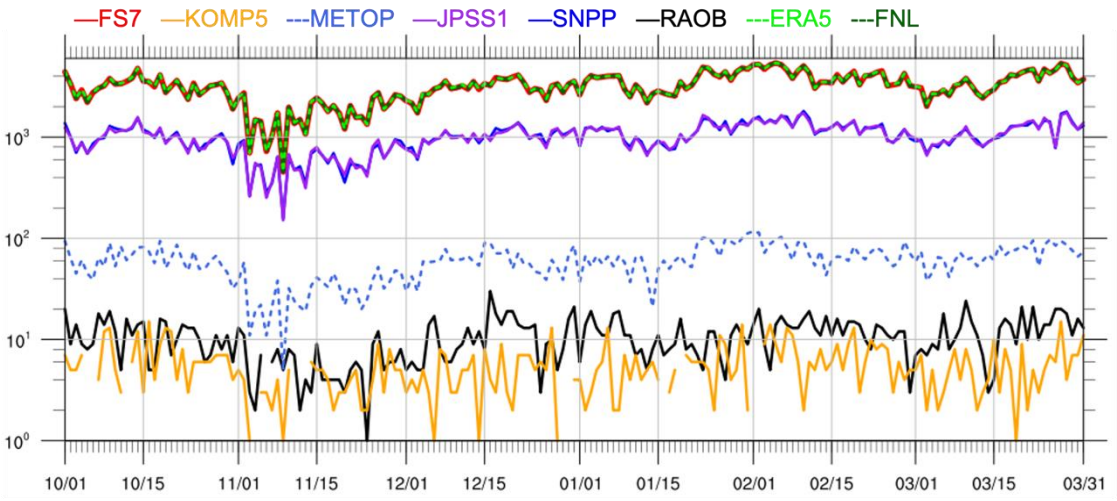

Figure 4. Daily data amounts during October 2019–March 2020 for FS7 (red), KOMP5 (orange), METOP (dash blue), JPSS1 (violet), SNPP (blue), RAOB (black), ERA5 (dash green), and FNL (dash dark green).

3. Analysis Results and Discussions

3.1. Spatiotemporal sensitivity

For the comparison between FS7 RO data and other datasets, the effect of spatiotemporal distance on the analysis should be examined for collocated RO points. Figure 5 shows the statistical spatial difference between FS7 and different datasets, including radiosonde (RAOB), both global analyses (ERA5 and FNL), other RO missions (METOP and KOMP5), and satellite retrievals (JPSS1 and SNPP). The absolute differences were averaged from surface to 200 hPa. For both temperature and vapor pressure, the analysis is not sensitive to temporal departure between any data pairs within 3 h (Figure 5a,b). The magnitude of the absolute mean difference in temperature is largest for RAOB, followed by satellite retrievals, other RO missions, and then the global analyses (Figure 5a), but with smaller absolute mean differences in vapor pressure for satellite retrievals and KOMP5 (Figure 5b). The spatial comparison for KOMP5 might have high uncertainty because of the fewer data collocations (Figure 4). The magnitude and ranking of the absolute mean difference in temperature for different datasets are similar, regardless of temporal departure and spatial distance. The ranking for different datasets is also the same in comparison for water vapor pressure, except for the METOP and KOMP5. METOP and KOMP5 have the maximum and minimum differences, respectively, in vapor pressure. The temperature difference increases with the spatial distance for all the datasets, especially at a larger tendency of about 0.05 K per 100 km for both global analyses (NCEP FNL and ERA5). In contrast, there is only a small tendency for satellite retrievals (JPSS1 and SNPP). The tendency in vapor pressure difference for all the datasets is similar to that in temperature, but both satellite retrievals give nearly the same smallest deviations from the RO data. Generally, the value of the absolute mean difference in the 100 km range is comparable to the results of time departure, which is insensitive. To reduce the influences from temporal and spatial departures on the comparison, we adopted a spatiotemporal window of $\pm$3 h and $\pm$100 km for the collocated RO points. The wet retrieval from RO measurement in principle is the averaged state along the ray point and, in general, will be closer to satellite retrievals and global analyses at a relatively coarser resolution but deviated more much from RAOB (as point measurement). Since water vapor is generally less homogeneous than temperature in the lower troposphere, the larger deviation from the RO vapor pressure is present for radiosondes, as seen in Figure 5d. As discussed in [24], the METOP refractivity has a negative bias in the lower troposphere and reaches a maximum in the tropical region, which is where

the FS7 covers. The larger difference in the lower troposphere could translate to the retrieved vapor pressure, which might be the reason for the larger difference for METOP in Figure 5d.

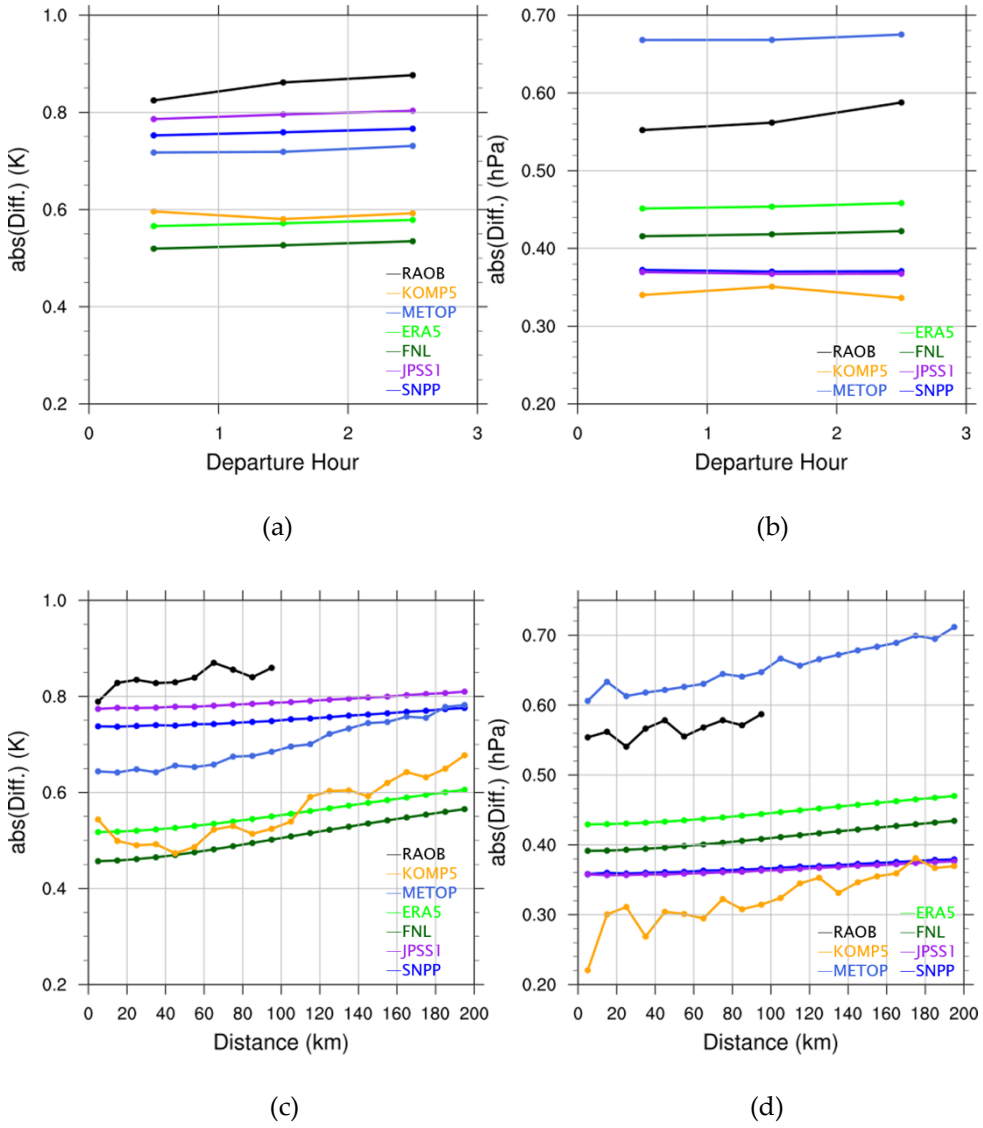

Figure 5. The mean absolute difference between FS7 and different datasets, including RAOB (black), KOMP5 (orange), METOP (light blue), ERA5 (green), FNL (dark green), JPSS1 (violet), and SNPP (blue), in (**a**) temperature (K) and (**b**) vapor pressure (hPa) versus the time (departure hours from the RO event) during October 2019–March 2020. The differences are averaged from surface to 200 hPa. (**c**,**d**) are as in (**a**,**b**), respectively, but versus the horizontal distance (in km) from the collocated RO point.

3.2. Ground-Truth Verifications

Before the comparisons with multiple datasets, more accurate independent observations should be used to quantify the data quality of FS7 wet RO retrievals. RAOB as a ground-truth measurement is useful for verification as described in [10], despite few being available over the ocean. For verification on oceanic RO soundings, the Central Weather Bureau (CWB) took two flights to obtain the in situ observations with DROP, which were released at times closer to the occurrence of RO soundings. The DROP was released east of Taiwan on 18 and 20 October 2019, as indicated in Figure 6. There are five FS7 RO profiles closer to the nine DROP, which are chosen for comparison. To assess the data quality of FS7, RAOB and DROP were taken as ground-truth observations. The reference data in Equation (1) were changed to RAOB or DROP for the FS7 RO data verification.

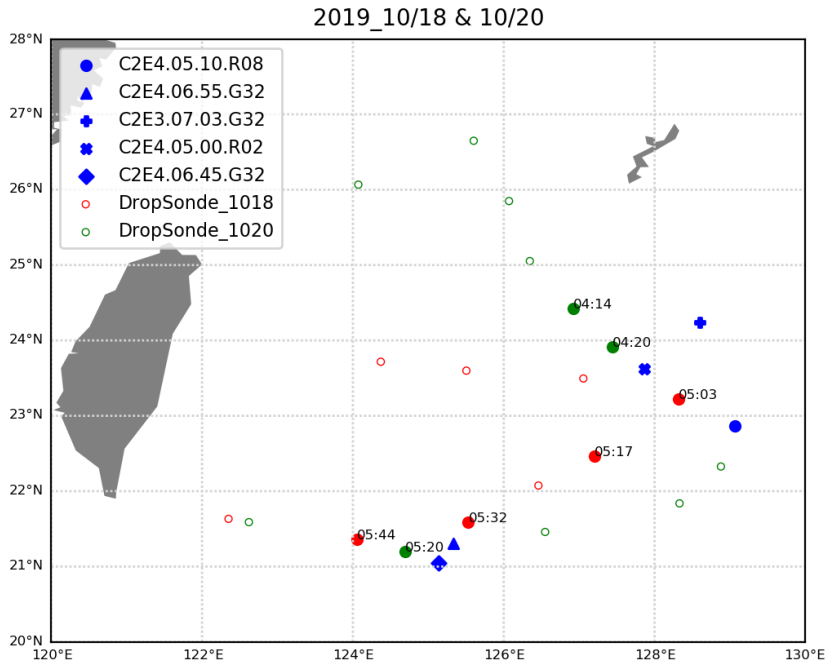

Figure 6. Locations of FS7 RO soundings (blue) and DROP on 18 (red) and 20 (green) October 2019. The red and green solid dots are the released DROP in the mission collocated with the five RO points, respectively, and the other DROP locations (open circles) were not used. The released time (UTC) of each collocated DROP is indicated by the numbers near the symbol.

There is a total of nine pairs for comparison after selecting both data that satisfy the time and distance criteria. Figure 7 show each comparison for vapor pressure and temperature. The spatial distances between the locations of the compared RO and DROP at different vertical levels are also presented. Most of the FS7 RO information extended to near-surface. As can be seen, both data exhibit very close temperatures in some pairs (Figure 7a–e) while also giving distinguishable differences in some pairs (Figure 7f–i) that are located over the region where Typhoon Neoguri is active near Okinawa at the time. The data pair in Figure 7e provides the smallest spatial distance between the DROP and FS7 RO soundings, generally less than 70 km. For this pair, the temperature and vapor pressure between RO and DROP are quite small, with small deviations within ± 1 °C and ± 1 hPa above 3 km, respectively. The statistical mean difference and STD for the nine data pairs are very small above 6 km height (Figure 7j). It shows a maximum temperature difference of 2 °C near 4 km height and a maximum positive vapor pressure difference of 2 hPa below 2 km. The temperature difference near the level of 4 km is larger than the 6-monthly statistics, which could be caused by the sample size and larger atmospheric variations associated with the typhoon system. In general, the temperature deviations are rather small in the upper troposphere for FS7 as in similar comparisons for FS3 (e.g., [7]), and the moisture deviations are about 2 hPa in the boundary layer regardless of the pair comparison.

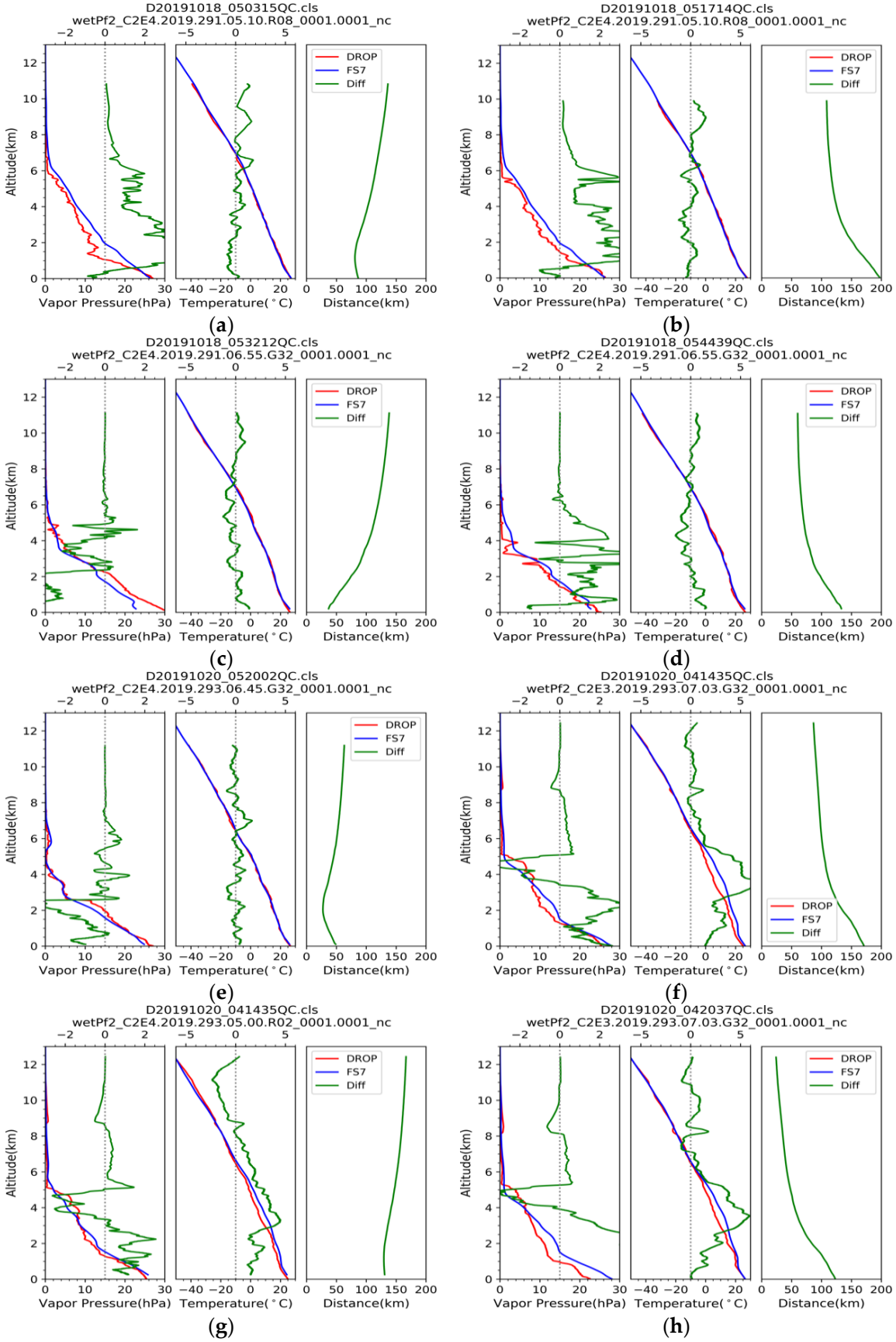

Figure 7. *Cont.*

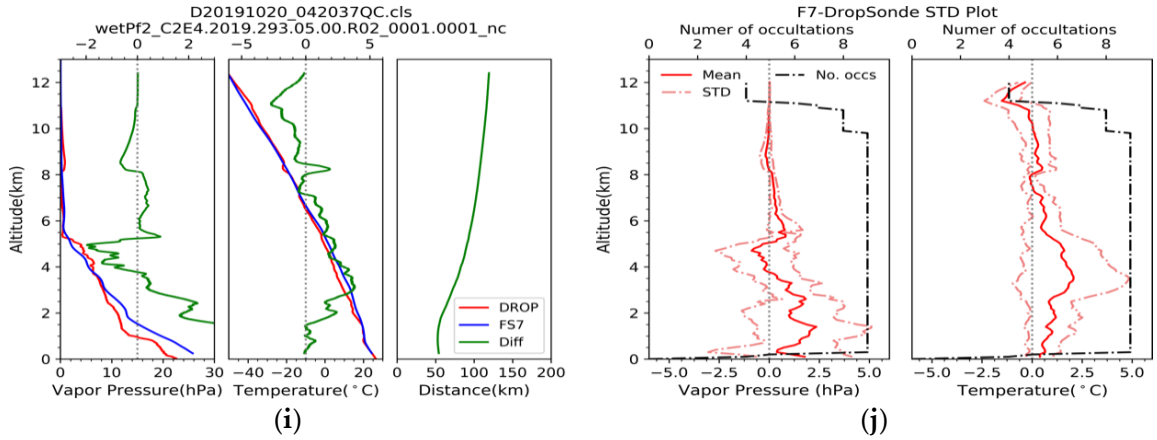

Figure 7. (**a**–**i**) The comparison between FS7 (blue) and DROP sounding (red), and their difference (green) in vapor pressure (hPa) and temperature (°C) on the left and middle of each panel. The right column on each panel shows the spatial distance between FS7 and DROP. (**j**) shows the mean difference and standard deviation (STD) averaged from the nine data pairs in (**a**–**i**).

Figure 8 shows similar comparisons with the radiosonde soundings that were released at different times in 2019 and 2020 from the Research Vessel Legend. The route of the Legend vessel travels between Dongsha Island and Taiping Island in the SCSTIMX (South China Sea Two Island Monsoon Experiment). There were two trips southwest of Taiwan, one from 24 to 26 August 2019 and the other from 14 to 16 April 2020, to release the radiosondes for comparison with FS7 RO data. There were in total eight pairs selected for the collocated comparison indicated in the figure. The temperature differences of FS7 data were further reduced in these pairs compared to Figure 7, with an average of about 0.5 °C deviation and STD throughout the troposphere (Figure 9i). On the other hand, FS7 RO data give less moisture than radiosonde below 2 km in most pairs and a negative mean difference of about 1 hPa within the troposphere (Figure 9i). However, the negative mean difference extended to −4 hPa near the surface over this region, which is somewhat larger than the corresponding value found to the east of Taiwan (Figure 7j).

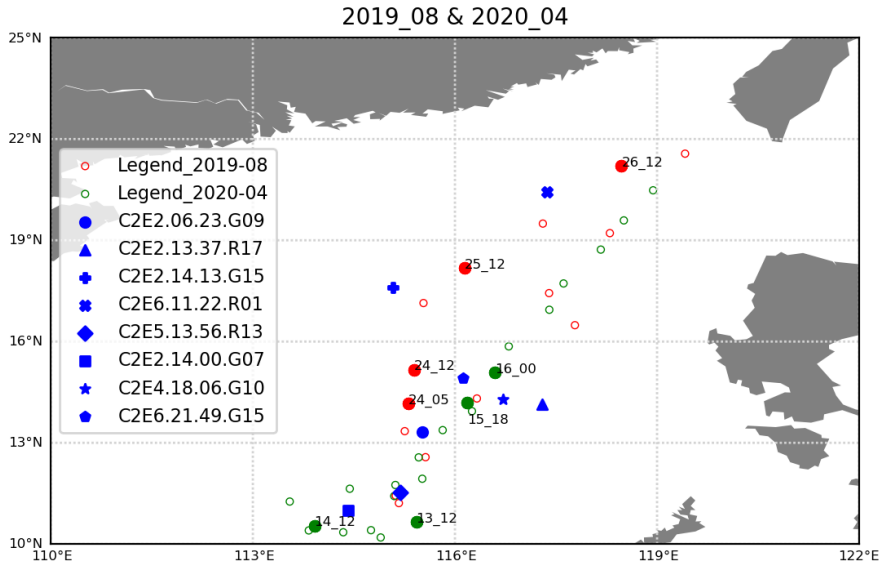

Figure 8. The same as that in Figure 6 but for the locations of FS7 RO soundings (blue) and RAOB released from the Research Vessel Legend on 24–26 August 2019 (red) and 14–16 April 2020 (green).

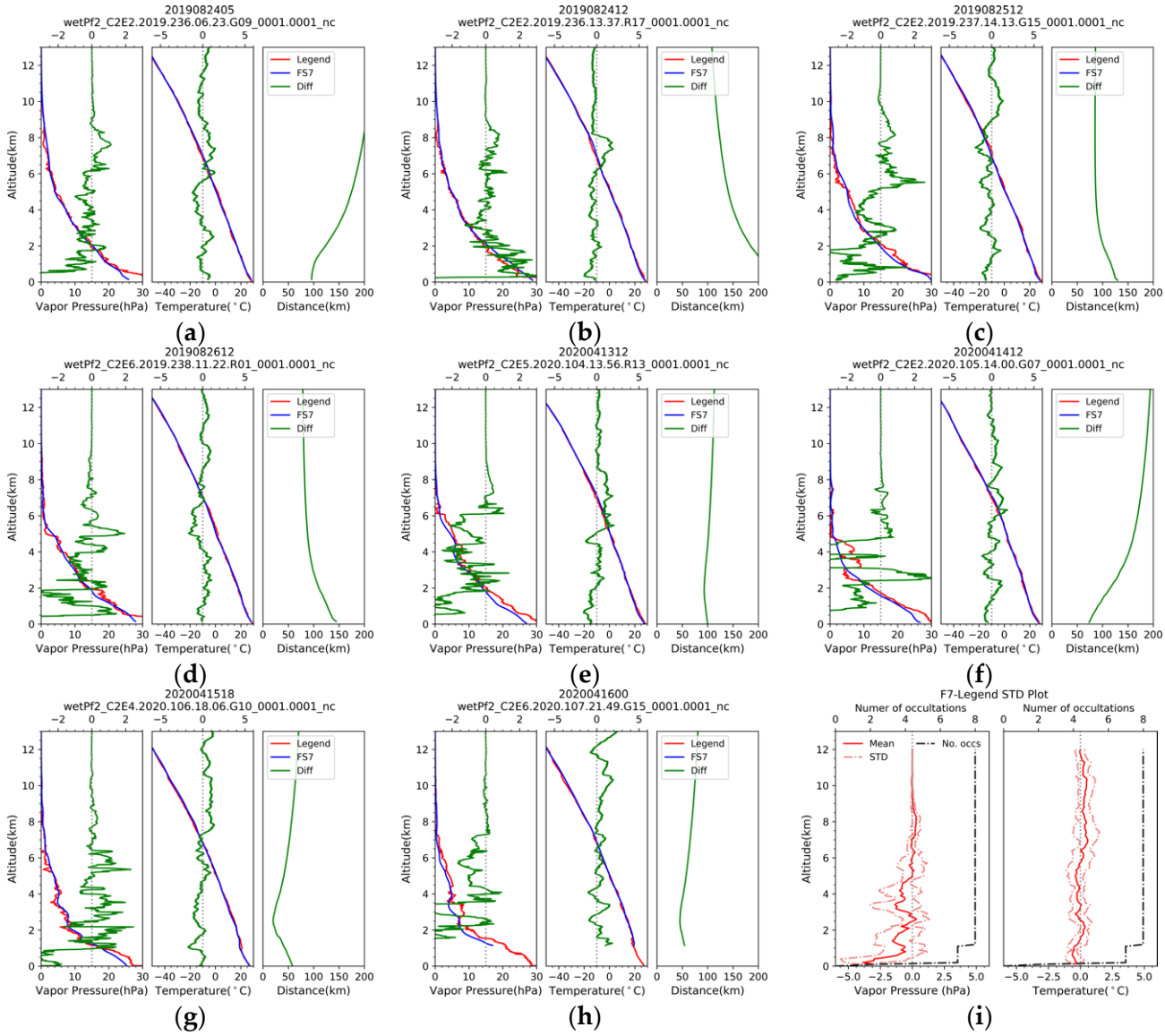

Figure 9. The same as that in Figure 7 but for the comparison between FS7 and RAOB released from the Research Vessel Legend. (**i**) is the mean difference and STD averaged from the eight data pairs in (**a**–**h**).

Besides the individual comparisons from the two chartered missions, the six-month data verification against RAOB was examined. The vertical distribution of the collocated data amounts of RAOB show no change between 2 km and 15 km and a quick decrease below about 2 km (Figure 10), and the volume gradually decreases above 16 km (figure not shown). In the troposphere, the six-month RAOB verifications show slightly positive differences in temperature and vapor pressure above 4 km but larger negative differences in vapor pressure in the lower troposphere. In the lower troposphere, RAOB has maximum deviations of about 1.5 °C and 2.2 hPa from the FS7 RO temperature and vapor pressure, respectively. A negative difference up to − hPa in the lower troposphere is present for RAOB, and the negative moisture deviation below 2 km is in agreement with the verification in [10], which may be associated with the tracking uncertainty due to the super-refraction from FS7 [7,9,10]. Generally, the absolute magnitudes of temperature and vapor pressure differences are less than 0.5 °C and 1 hPa, respectively, in the troposphere. The vertical average of the difference and STD from surface to 15 km altitude are 0.14 °C and 0.12 °C for temperature and are −0.03 hPa and 0.24 hPa for vapor pressure.

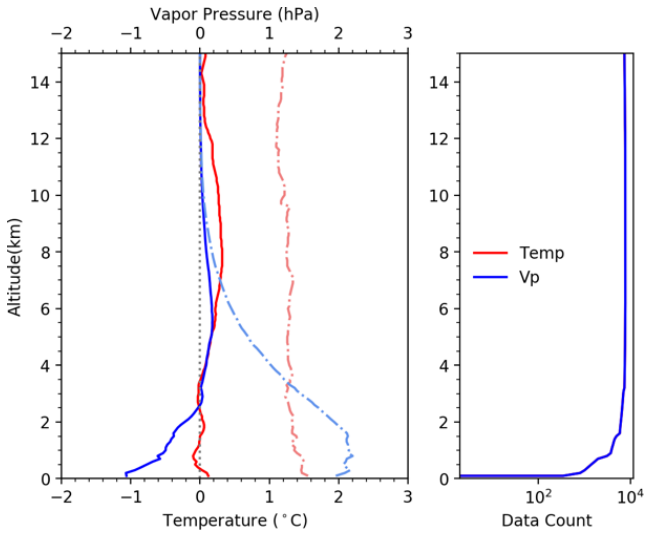

Figure 10. The mean differences (solid line) and standards deviation (STD, dashed line) between FS7 and RAOB in (**a**) temperature (°C, red) and (**b**) water vapor pressure (hPa, blue). The right panel shows vertical variations in the total counted data in comparison.

3.3. Verification against FS7

The analysis above showed the precision of FS7 with RAOB, and then, the FS7 data were derived as the reference data for multiple datasets. The vertical distribution of the collocated data amounts, METOP and KOMP5, are similar with no change between 2 km and 40 km but with the smallest amounts (several hundred to one thousand) for KOMP5 (Figure 11). The comparisons with the two datasets exhibit similar patterns in the troposphere, with negative differences in temperature and vapor pressure above 4 km. In the lower troposphere, both METOP and KOMP5 show positive differences in vapor pressure. Relatively larger differences are given by METOP in both temperature and moisture, with maxima of −0.5 °C and 2 hPa, respectively. For the temperature comparison (Figure 11a), KOMP5 shows the differences within 0.25 °C, which is about half of that for METOP. In the lower troposphere, KOMP5 also shows a small deviation from the FS7 RO temperature. On the other hand, the differences in vapor pressure increase from KOMP5 to Metop (Figure 11b). The mean difference between FS7 and KOMP5 shows very small magnitudes at all vertical levels, except with some amounts less than 0.5 hPa below 2 km. In contrast, METOP gives a larger vapor pressure difference when compared with FS7, which may associate with the larger refractivity bias in lower troposphere for METOP, as discussed in Section 3.1. On the other hand, the KOMP5 data downloaded from TACC, which use the same retrieval algorithm as used for FS7, thus has generally smaller mean differences and STDs for both temperature and vapor pressure, which is in better agreement with FS7.

Figure 12 shows the differences in the analyses between FS7 and other datasets, including ERA5, FNL, JPSS1, and SNPP. The amounts of data pairs for comparison are almost constant with height but are gradually reduced from 700 hPa to 1000 hPa. Compared to both FNL and ERA5, the temperature differences show negative differences for most of the profiles from surface to 200 hPa (Figure 12a). However, the comparison with satellite retrievals (JPSS1 and SNPP) show positive temperature differences below about 4 km (600 hPa) and larger negative differences relative to the global analyses above this height. The maximum temperature bias is about −0.6 K at about 450 hPa. The comparisons with global analyses exhibit smaller mean temperature differences and STDs, about half of those for both the satellite data. Even though FS7 RO analysis shows larger mean temperature differences and STD in comparison with satellite retrievals (Figure 12a), their absolute magnitudes are still comparable with those from other RO soundings or radiosondes, as shown in Figures 10 and 11a. For vapor pressure (Figure 12b), both FNL and ERA5

show positive differences within 1 hPa near the surface. FNL gives a relatively smaller mean difference than ERA5, which might be associated with the fact that the NCEP short-term forecast is used as the model first gauss for the 1DVAR retrieval [25]. Thus, the verifications against FNL show the smallest STDs in both temperature and vapor pressure. In comparison with JPSS1 and SNPP in moisture, negative mean differences of about −0.5 hPa in 600–900 hPa are present in Figure 12b. The mean differences in both temperature and vapor pressure for both satellite retrievals are opposite to those for both global analyses below about 4 km (600 hPa) (Figure 12). As shown in Figures 5 and 12, the JPSS1 and SNPP have similar patterns when compared to FS7, and the two datasets are combined together as NUCAPS for the later comparison.

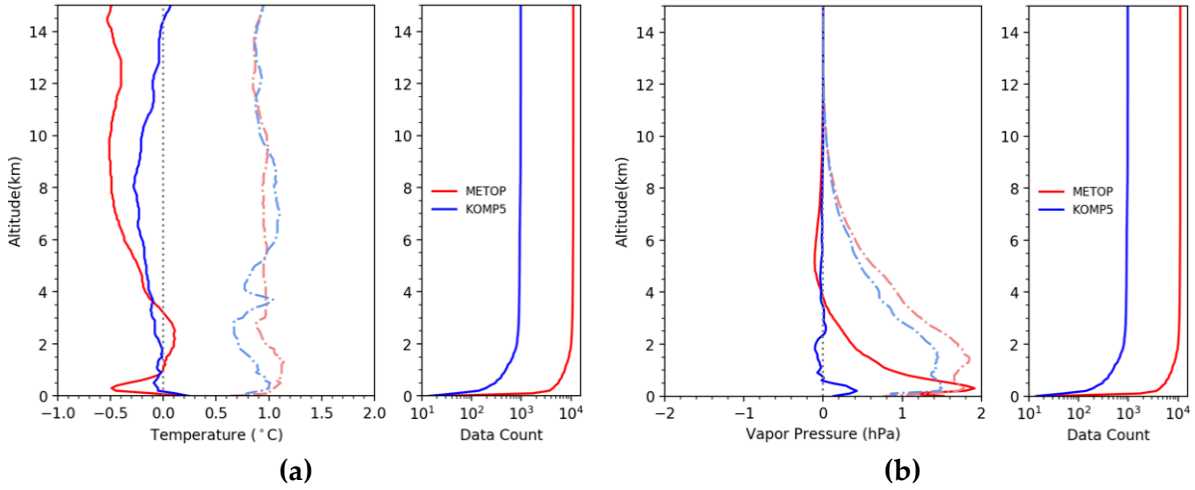

Figure 11. The mean differences (solid line) and standard deviations (STD, dashed line) between FS7 and different datasets, including METOP (red) and KOMP5 (blue), in (**a**) temperature (°C) and (**b**) water vapor pressure (hPa). The right panel shows the vertical variations of the total counted data in comparison.

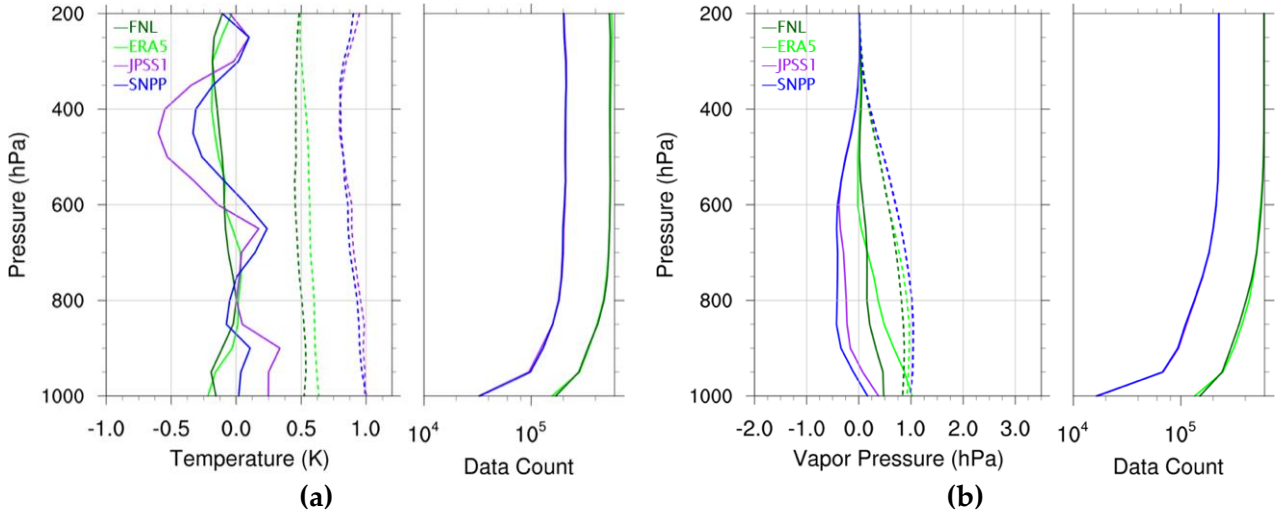

Figure 12. The same as that in Figure 11 but between FS7 and different datasets, including ERA5 (green), FNL (dark green), JPSS1 (violet), and SNPP (blue) along the pressure coordinate.

The latitudinal distributions of the mean differences between FS7 RO data and ERA5, FNL, and NUCAPS are shown in Figure 13. The mean differences and STDs are longitudinally averaged for their latitudinal distributions. For FNL and ERA5, the mean temperature differences are roughly similar, with slightly larger negative values in the tropical region below about 1 km altitude (900 hPa) as well as comparable negative values throughout

the latitudinal bins in the upper troposphere. Most of the temperature differences are within −0.2 K for ERA5 and FNL and exhibit much smaller magnitudes roughly in the middle troposphere (Figure 13a,c). The comparison indicates that ERA5 may be impacted with larger cold biases in the boundary layer near the equator than FNL if FS7 RO wet temperature is deemed more reliable. For vapor pressure, it is noted that positive mean differences appear throughout the latitude and below about 5 km (500 hPa) (Figure 13b,d), and the deviations from ERA5 in the tropical region are somewhat larger than from FNL. For NUCAPS, the temperature and moisture deviations from FS7 are quite different from those obtained with both global analyses (Figure 13e,f). For example, there are significant temperature differences of around −0.5 K in 300–600 hPa, while presenting positive differences mainly in 600–700 hPa and 900–1000 hPa. Furthermore, most of the moisture differences are negative below about 6 km altitude (400 hPa) throughout the latitude. Since the larger moisture differences for the satellite retrievals are opposite to those for both global analyses, FS7 RO data may suggest a bias possibly existing in the water vapor retrieval of NUCAPS [26]. A dry bias of water vapor retrieval from NUCAPS was revealed in [27,28] due to the absorption of clouds in the infrared spectrum.

Figure 14 shows the mean differences and STDs within ±45° latitudes for different datasets, which are vertically averaged between 200 and 1000 hPa. Negative temperature differences are present over most of the plotted regions, with weaker magnitudes over different regions for different datasets that are not revealed from the latitudinal distributions in Figure 13. Larger deviations are found near the tropical region where contains more active convection in the intertropical convergence zone (ITCZ) (Figure 14a,c). Differing from the comparison with ERA5 and FNL, the temperature differences for NUCAPS are relatively smaller near the equator but somewhat larger outside (Figure 13e). The deviations have larger variations along the latitude for NUCAPS, with a dramatic change to a maximum of −0.05 K near the equator and a minimum of −0.2 K in some regions near ±45°. The apparent deviation with colder temperature for FNL is contributed by larger magnitudes extended along the equatorial regions, mainly from Africa to the Western Pacific. For both ERA5 and FNL, the STDs of their temperature differences are below 0.2 K in the tropical region (Figure 14b,d), significantly smaller than those for NUCAPS, which is also evident in their zonal average and meridional average. The temperature differences over the tropical region are generally larger over the land than over the ocean for the three datasets. There are particularly large deviations in STD over Tibet for NUCAPS. All three datasets exhibit smaller STDs in lower latitudes, with no common in-phase signal in longitudes.

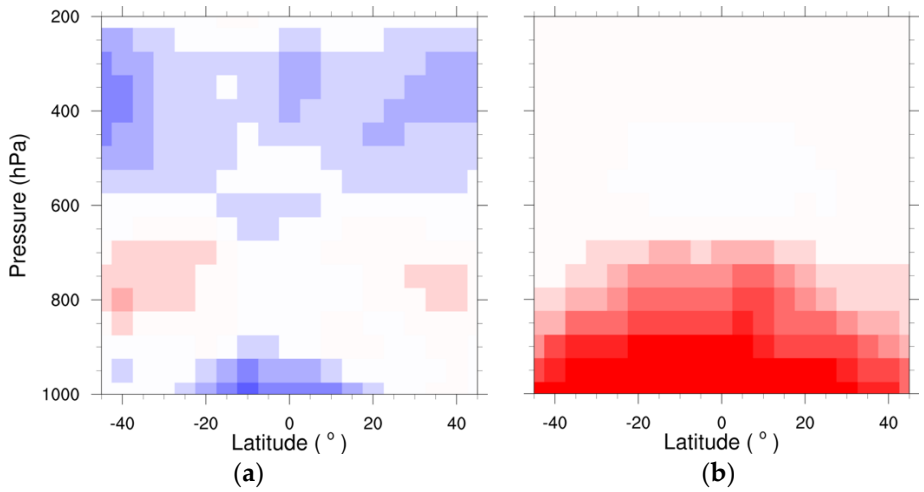

Figure 13. *Cont.*

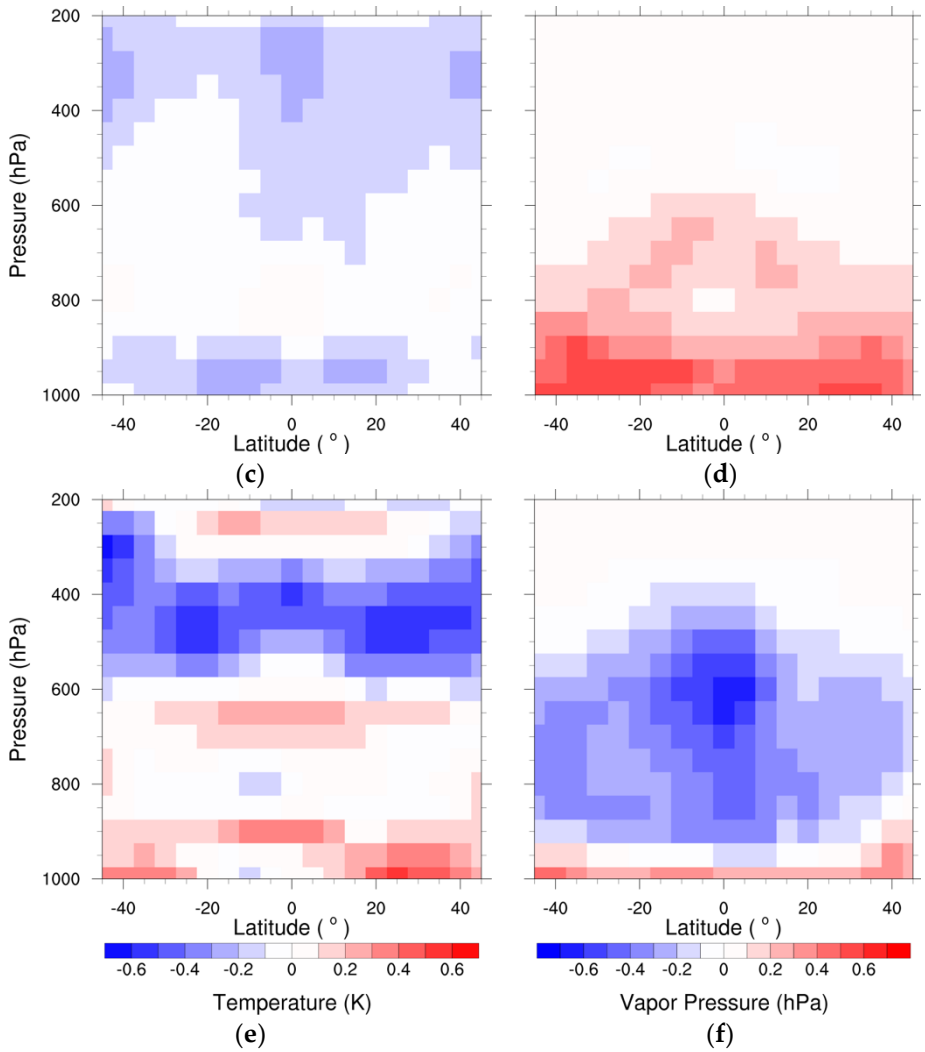

Figure 13. Pressure–latitude cross section of mean differences between FS7 and ERA5 averaged in a 10° by 10° bin in (**a**) temperature (K) and (**b**) vapor pressure (hPa). (**c**,**d**) are as in (**a**,**b**) but for FNL, respectively. (**e**,**f**) are as in (**a**,**b**), respectively, but for NUCAPS (JPSS1 and SNPP), respectively.

For vapor pressure, as shown in Figure 15, positive mean differences are produced when compared to both ERA5 and FNL, with somewhat larger magnitudes mainly in the lower latitudes for the former (Figure 15a). For FNL, the deviations are reduced below 0.2 hPa in the tropical region (Figure 15c) compared to those of ERA5 with 0.3 hPa (Figure 15a), which is also indicated by their zonal average. The water pressure differences for NUCAPS show significantly larger positive values with a minimum of −0.5 hPa, mainly near the equator (Figure 15e) in opposition to those of both global datasets. In terms of STD, ERA5 also gives larger deviations than FNL, but mainly over the southern hemisphere; both are much smaller than that for NUCAPS (Figure 15f). More consistency with both global analyses tend to suggest that some biases may be associated with NUCAPS retrievals, and FS7 retrievals may provide a reference to the bias correction for NUCAPS. In this study, only overall salient differences in the comparisons with three datasets are focused and without further detailing irregular variations with latitude or longitude.

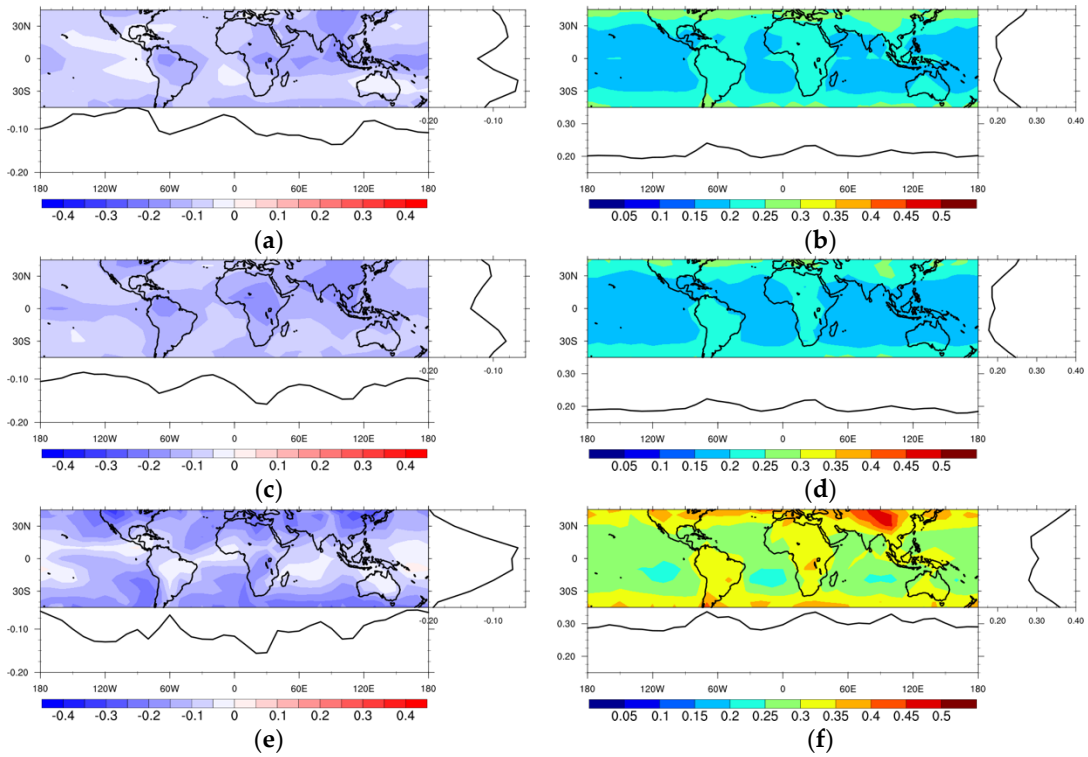

Figure 14. The mean differences between FS7 and different datasets including (**a**) ERA5, (**c**) FNL, and (**e**) NUCAPS in temperature (K). (**b**,**d**,**f**) are as in (**a**,**c**,**e**), respectively, but for STD. Both mean differences and STDs are averaged in the surface to 200 hPa. Curves to the right and bottom of each panel show the zonal average and meridional average of the analysis, respectively.

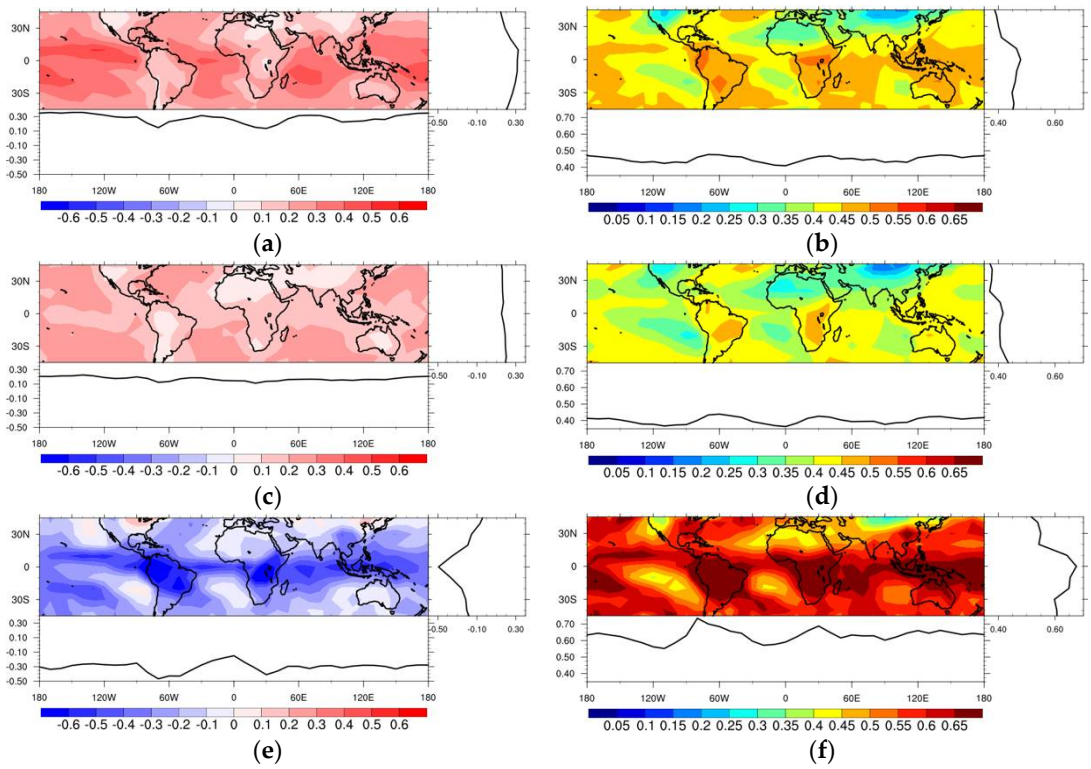

Figure 15. The same as that in Figure 14 but for vapor pressure (hPa), which is averaged from the surface to 500 hPa.

4. Conclusions

FS7 project is the follow-on mission of FS3, consisting of six satellites in the low inclination of 24° that were launched in June 2019. The RO observation data of FS7 was officially released at the end of 2019. With the ability to receive signals from both GPS and GLONASS, and the high SNR, FS7 can provide more RO data amounts (up to 5000 per day) and further penetrative depth into the lower troposphere than FS3. The analysis results show that the rate of penetration below 1 km is about 40% for FS3 but can reach 80% for FS7.

Two chartered missions providing airborne and ship soundings from dropsondes and radiosondes are used for verification on FS7 RO data retrievals. The comparisons with chartered sounding observations over two oceanic regions east and southwest of Taiwan present a good consistency between FS7 and soundings from dropsondes and radiosondes when data pairs are collocated with each other. The mean differences and STDs for FS7 RO data are in agreement with the 6-month (Oct. 2019–Mar. 2020) statistics, which were verified against operational radiosondes. These comparisons support the small deviations in FS7 temperature in the troposphere, generally less than 0.5 °C. Negative biases in vapor pressure are present in the lower troposphere with a typical magnitude near 2 hPa and may double near the surface for some comparisons. The negative biases at the lower troposphere may be associated with RO refractivity.

In this study, we also compared the RO data retrievals of FS7 with multiple datasets, including the RO products from the EUMETSAT Metop-A/B/C and Korean KOMPSAT-5, global analyses from ERA5 and NCEP FNL, and satellite retrievals from NUCAPS. With a spatiotemporal window of ±3 h and ±100 km, the comparisons with multiple datasets against FS7 within ±45° latitude in the selected period of six months exhibit consistent patterns in the troposphere with negative differences in temperature and positive differences on vapor pressure except for the NUCAPS data. Generally, the deviations and STDs of temperature for FS7 are less than 0.5 °C and 1.0 °C, respectively. For vapor pressure, they are generally within ±2 hPa. Comparisons with NUCAPS retrievals show mean differences opposite to those from both global analyses and other sounding data. From the latitudinal distributions of mean difference and STD, the ITCZ is evident from the comparisons, especially for NUCAPS, which shows a larger deviation in moisture when compared to FS7/C2 RO data.

In this study, the comparisons completely rely on the RO wet products at TACC, which are retrieved by the 1DVAR algorithm. It is interesting to identify whether the moisture at lower levels may be better retrieved with data assimilation of the RO bending angle in the future. On the other hand, the comparisons from the statistics and two chartered observational missions highlighted the potential usefulness of the RO-retrieved moisture from FS7 for analysis of the marine boundary layer. Future study might consider the impacts due to the clouds (e.g., [29,30]) so that the uncertainties could be further consolidated for additional factors.

Author Contributions: Conceptualization, S.-Y.C., C.-Y.L. and C.-Y.H. (Ching-Yuang Huang); Data curation, P.-H.L., J.-P.C. and C.-Y.H. (Cheng-Yung Huang); Formal analysis, S.-Y.C., C.-Y.L. and C.-Y.H. (Ching-Yuang Huang); Project administration, S.-Y.C., C.-Y.L. C.-Y.H. (Ching-Yuang Huang) and C.-Y.H. (Cheng-Yung Huang); Software, C.-Y.L., S.-C.H. and H.-W.L.; Validation, C.-Y.L, S.-Y.C., S.-C.H. and H.-W.L.; Writing—original draft, S.-Y.C.; Writing—review & editing, S.-Y.C., C.-Y.L. and C.-Y.H. (Ching-Yuang Huang). All authors have read and agreed to the published version of the manuscript.

Funding: This research was funded jointly by the Ministry of Science and Technology (MOST) (grant No. MOST 109-2111-M-008-026-) and National Space Organization (NSPO) (grant No. NSPO-S-109138) in Taiwan.

Institutional Review Board Statement: Not applicable.

Informed Consent Statement: Not applicable.

Data Availability Statement: Publicly available datasets were analyzed in this study. The repositories of the datasets have been indicated in the text.

Acknowledgments: The authors would like to thank Shu-Hui Ho, Jyun-Ying Huang, and Ching-Chieh Lin at Taiwan Analysis Center for COSMIC (TACC) for providing FS7/C2 RO data, and Kang-Ning Huang at Central Weather Bureau (CWB) in Taiwan for providing dropsonde data.

Conflicts of Interest: The authors declare no conflict of interest.

References

1. Ho, S.-P.; Anthes, R.A.; Ao, C.O.; Healy, P.S.; Horanyi, A.; Hunt, D.; Mannucci, A.J.; Pedatella, N.; Randel, W.J.; Simmons, A.; et al. The COSMIC/FORMOSAT-3 radio occultation mission after 12 years. *Bull. Am. Meteorol. Soc.* **2020**, *101*, E1107–E1136. [CrossRef]
2. He, W.; Ho, S.-P.; Chen, H.; Zhou, X.; Hunt, D.; Kuo, Y. Assessment of radio-sonde temperature measurements in the upper troposphere and lower strato-sphere using COSMIC radio occultation data. *Geophys. Res. Lett.* **2009**, *36*, L17807. [CrossRef]
3. Pirscher, B.; Foelsche, U.; Borsche, M.; Kirchengast, G.; Kuo, Y.-H. Analysis of migrating diurnal tides detected in FORMOSAT-3/COSMIC temperature data. *J. Geophy. Res.* **2010**, *115*, D14108. [CrossRef]
4. Xie, F.; Wu, D.L.; Ao, C.O.; Kursinski, E.R.; Mannucci, A.J.; Syndergaard, S. Super-refraction effects on GPS radio occultation refractivity in marine boundary layers. *Geo. Res. Lett.* **2010**, *37*, L11805. [CrossRef]
5. Ho, S.-P.; Hunt, D.; Steiner, A.K.; Mannucci, A.J.; Kirchengast, G.; Gleisner, H.; Heise, S.; von Engeln, A.; Marquardt, C.; Sokolovskiy, S.; et al. Reproducibility of GPS radio occultation data for climate monitoring: Profile-to-profile inter-comparison of CHAMP climate records 2002 to 2008 from six data centers. *J. Geophys. Res.* **2012**, *117*, D18111. [CrossRef]
6. Chu, C.-H.; Fong, C.-J.; Xia-Serafino, W.; Shiau, A.; Taylor, M.; Chang, M.-S.; Chen, W.-J.; Liu, T.-Y.; Liu, N.-C.; Martins, B.; et al. An Era of Constellation Observation- FORMOSAT-3/COSMIC and FORMOSAT-7/COSMIC-2. *J. Aeronaut. Astronaut. Aviat.* **2018**, *50*, 335–346.
7. Schreiner, W.S.; Weiss, J.P.; Anthes, R.A.; Braun, J.; Chu, V.; Fong, J.; Hunt, D.; Kuo, Y.-H.; Meehan, T.; Serafino, W.; et al. COSMIC-2 radio occultation constellation: First results. *Geo. Res. Lett.* **2020**, *47*, e2019GL086841. [CrossRef]
8. Kuo, Y.H.; Wee, T.K.; Sokolovskiy, S.; Rocken, C.; Schreiner, W.; Hunt, D.; Anthes, R.A. Inversion and error estimation of GPS radio occultation data. *J. Meteor. Soc. Jpn.* **2004**, *82*, 507–531. [CrossRef]
9. Anthes, R.A.; Bernhardt, P.A.; Chen, Y.; Cucurull, L.; Dymond, K.F.; Ector, D.; Healy, S.B.; Ho, S.-P.; Hunt, D.C.; Kuo, Y.-H.; et al. The COSMIC/FORMOSAT-3 Mission: Early results. *Bull. Amer. Meteor. Soc.* **2008**, *89*, 313–333. [CrossRef]
10. Ho, S.-P.; Zhou, X.; Shao, X.; Zhang, B.; Adhikari, L.; Kireev, S.; He, Y.; You, J.G.; Xoa-Serafino, W.; Lynch, E. Initial Assessment of the COSMIC-2/FORMOSAT-7 Neutral Atmosphere Data Quality in NESDIS/STAR Using In Situ and Satellite Data. *Remote Sens.* **2020**, *12*, 4099. [CrossRef]
11. NCEP GDAS/FNL 0.25 Degree Global Tropospheric Analyses and Forecast Grids. Available online: https://rda.ucar.edu/datasets/ds083.3/ (accessed on 1 April 2020).
12. Hersbach, H.; Bell, B.; Berrisford, P.; Biavati, G.; Horányi, A.; Muñoz Sabater, J.; Nicolas, J.; Peubey, C.; Radu, R.; Rozum, I.; et al. ERA5 hourly data on pressure levels from 1979 to present. In *Copernicus Climate Change Service (C3S) Climate Data Store (CDS)*; ECMWF; Available online: https://cds.climate.copernicus.eu/cdsapp#!/dataset/reanalysis-era5-pressure-levels?tab=overview (accessed on 16 February 2021). [CrossRef]
13. Loiselet, M.; Stricker, N.; Menard, Y.; Luntama, J.-P. GRAS-Metop's GPS-based atmospheric sounder. *Esa Bull.* **2020**, *102*, 38–44.
14. von Engeln, A.; Healy, S.; Marquardt, C.; Andres, Y.; Sancho, F. Validation of operational GRAS radio occultation data. *Geophys. Res. Lett.* **2009**, *36*, L17809. [CrossRef]
15. Schreiner, W.; Sokolovskiy, S.; Hunt, D.; Rocken, C.; Kuo, Y.-H. Analysis of GPS radio occultation data from the FORMOSAT-3/COSMIC and Metop/GRAS missions at CDAAC. *Atmos. Meas. Tech.* **2011**, *4*, 2255–2272. [CrossRef]
16. Weiss, J.; Ho, B.; Hoekstra, M.; Huelsing, H.; Hunt, D.; Rousseau, M.; Sleziak-Sallee, M.; Schreiner, B.; Sokolovskiy, S.; Vanhove, T.; et al. UCAR COSMIC data analysis and archive center (CDAAC) status and plans. In Proceedings of the 4th International Conference on GPS Radio and Occultation, Taipei, Taiwan, 18–20 April 2018.
17. Bowler, N.E. An initial assessment of the quality of RO data from KOMPSAT-5. *GRAS SAF Rep.* **2018**, *32*, 18.
18. Healy, S. ECMWF starts assimilating COSMIC-2 data. *Ecmwf Newsl.* **2020**, *163*, 5–6.
19. Shao, H.; Bathmann, K.; Zhang, H.; Huang, Z.-M.; Cucurull, L.; Vandenberghe, F.; Treadon, R.; Kleist, D.; Yoe, J.G. COSMIC-2 NWP assessment and implementation at JCSDA and NCEP. In Proceedings of the 5th International Conference on GPS Radio and Occultation, Taipei, Taiwan, 27–29 May 2020.
20. Gambacorta, A.; Barnet, C.D. Methodology and information content of the NOAA NESDIS operational channel selection for the Cross-Track Infrared Sounder (CrIS). *IEEE Trans. Geosci. Remote Sens.* **2012**. [CrossRef]
21. Wang, P.; Li, J.; Li, Z.; Lim, A.H.N.; Li, J.; Goldberg, M.D. Impacts of observation errors on hurricane forecasts when assimilating hyperspectral infrared sounder radiances in partially cloudy skies. *J. Geophys. Res.* **2019**, *124*, 10802–10813. [CrossRef]
22. Liu, C.-Y.; Kuo, S.-C.; Lim, A.H.N.; Hsu, S.-C.; Tseng, K.-H.; Yeh, N.-C.; Yang, Y.-C. Optimal Use of Space-Borne Advanced Infrared and Microwave Soundings for Regional Numerical Weather Prediction. *Remote Sens.* **2016**, *8*, 816. [CrossRef]

23. Liu, C.-Y.; Li, J.; Ho, S.-P.; Liu, G.-R.; Lin, T.-H.; Young, C.C. Retrieval of Atmospheric Thermodynamic State from Synergistic Use of Radio Occultation and Hyperspectral Infrared Radiances Observations. *IEEE J. Sel. Top. Appl. Earth Obs. Remote Sens.* **2016**, *9*, 744–756. [CrossRef]
24. Gorbunov, M.E.; Lauritsen, K.B.; Benzon, H.-H.; Larsen, G.B.; Syndergaard, S.; Sørensen, M.B. Processing of GRAS/METOP radio occultation data recorded in closed-loop and raw-sampling modes. *Atmos. Meas. Tech.* **2011**, *4*, 1021–1026. [CrossRef]
25. Poli, P.; Joiner, J.; Kursinski, E.R. 1DVAR analysis of temperature and humidity using GPS radio occultation refractivity data. *J. Geophy. Res.* **2002**, *107*, D20. [CrossRef]
26. Smith, N.; Barnet, C.D. Uncertainty Characterization and Propagation in the Community Long-Term Infrared Microwave Combined Atmospheric Product System (CLIMCAPS). *Remote Sens.* **2019**, *11*, 1227. [CrossRef]
27. Pu, Z.; Zhang, L. Validation of Atmospheric Infrared Sounder temperature and moisture profiles over tropical oceans and their impact on numerical simulations of tropical cyclones. *J. Geophy. Res.* **2010**, *115*, D24112. [CrossRef]
28. Zheng, J.; Li, J.; Schimit, T.J.; Li, J.; Liu, Z. The Impact of AIRS Atmospheric Temperature and Moisture Profiles on Hurricane Forecasts: IKE (2008) and Irene (2011). *Adv. Atmos. Sci.* **2015**, *32*, 319–335. [CrossRef]
29. Liu, C.-Y.; Chiu, C.-H.; Lin, P.-H.; Min, M. Comparison of Cloud-Top Property Retrievals from Advanced Himawari Imager, MODIS, CloudSat/CPR, CALIPSO/CALIOP, and radiosonde. *J. Geophys. Res. Atmos.* **2020**, *125*, e2020JD032683. [CrossRef]
30. Lasota, E.; Rohm, W.; Liu, C.-Y.; Hordyniec, P. Cloud Detection from Radio Occultation Measurements in Tropical Cyclones. *Atmosphere* **2018**, *9*, 418. [CrossRef]